

Microwave-Controlled Cold Chemistry

Fernanda B. V. Martins¹, Hansjürg Schmutz, Josef A. Agner, Valentina Zhelyazkova^{1,*}, and Frédéric Merkt¹
Institute of Molecular Physical Science, ETH Zürich, Zürich, Switzerland

 (Received 27 November 2024; accepted 5 February 2025; published 24 March 2025)

Ion-molecule reactions proceed with highly rotational-state-specific rate coefficients and are amenable to stereodynamical control at low temperatures. We introduce a scheme to control cold ion-molecule chemistry with microwaves based on the coherent transfer of molecular rotational-state populations. We use a merged-beam approach to reach collision energies in the range from ~ 0 to $k_B \times 10$ K for the reaction between He^+ and rotationally cold CO molecules ($T_{\text{rot}} \approx 3$ K) and manipulate the rotational-state population of CO using microwave pulses. We achieve reaction inhibition by up to $\sim 40\%$ with microwave pulses resonant with pure-rotational transitions in CO, unambiguously demonstrating a nonthermal mechanism for microwave-assisted chemistry.

DOI: 10.1103/PhysRevLett.134.123401

At low temperatures, gas-phase molecules occupy only very few quantum states and are sensitive to external fields and to long-range forces exerted by neighboring particles. These properties make it possible to experimentally manipulate their motion, their quantum states, and their chemical reactivity. As a result, cold molecules are exploited in a rapidly growing number of applications [1] including quantum information processing and simulation [2,3], metrology and fundamental physics [4,5], and cold chemistry [6–11].

In the context of cold chemistry, the topic of the present Letter, ion-molecule reactions play a special role: Long-range intermolecular forces between ions and molecules attract even distant partners. For barrier-free exothermic reactions, the attractive forces lead to reactive capture with high rate constants, particularly at low temperatures, which explains their dominance in rarefied chemical environments such as interstellar clouds [12–14].

The general theoretical framework to understand the key features of the state specificities and stereodynamics of low-temperature ion-molecule capture reactions, rotationally adiabatic capture theory [15–20], has been derived more than 30 years ago. It is, however, only recently that experiments have reached the low temperatures and the low collision energies needed to rigorously test the theoretical predictions [21–27]. Based on theory and experiments, it is now established that the inhomogeneous electric field emanating from the ion acts differently on different conformation isomers [28], different isotopologues [29–31], and different nuclear-spin isomers [11,20] of the neutral

molecules and even on their different rotational levels and magnetic sublevels [11,25,31–34].

In this Letter, we present new results on the control of cold ion-molecule reactions by microwave radiation with the example of the $\text{He}^+ + \text{CO} \rightarrow \text{He} + \text{C}^+ + \text{O}$ reaction. Specifically, we demonstrate the use of microwave pulses as switches between different levels of chemical reactivity through the coherent transfer of population between rotational states of the neutral molecule. The mechanism for the microwave control of low-temperature reactivity is illustrated in Fig. 1. It relies on (i) the large differences in the capture rate coefficients associated with the different $|J, M_J\rangle$ rotational levels of CO [33] [Fig. 1(a)], (ii) the large imbalance of the occupation probability of the lowest rotational levels of CO below $T_{\text{rot}} \approx 5$ K, and (iii) the microwave-induced coherent population transfer (π pulse) between pairs of rotational levels [Figs. 1(b)–1(d)].

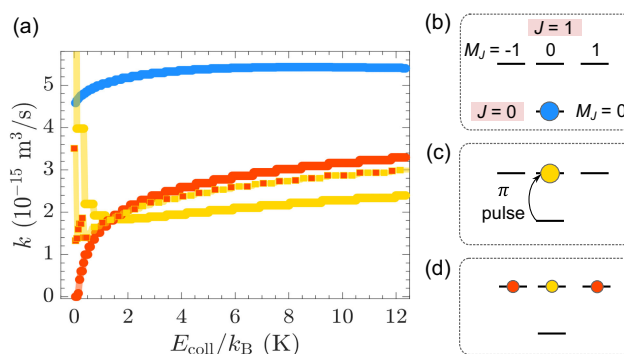


FIG. 1. (a) Rotational-state-specific capture rate coefficients of the $\text{He}^+ + \text{CO}(|J, M_J\rangle) \rightarrow \text{He} + \text{C}^+ + \text{O}$ reaction for $|J, M_J\rangle = |0, 0\rangle$ (blue), $|1, 0\rangle$ (yellow), $|1, \pm 1\rangle$ (orange) and for a statistical average of $|1, -1\rangle$, $|1, 0\rangle$, and $|1, 1\rangle$ (orange-yellow dashed line) from Ref. [33]. (b)–(d) Illustration of the microwave-induced coherent population transfer between the $|0, 0\rangle$ (b) and $|1, 0\rangle$ (c) states of CO and after randomization of M_J (d).

*Contact author: valentina.zhelyazkova@phys.chem.ethz.ch, valentina.zhelyazkova@ucl.ac.uk

Present address: Department of Physics and Astronomy, University College London, Gower Street, London WC1E 6BT, United Kingdom.

For simplicity of the argument, we consider first the case where only the ground $|0,0\rangle$ level is populated [see Fig. 1(b)]. In the collision-energy (E_{coll}) range of interest (E_{coll}/k_B between 100 mK and 12 K), this level [blue trace in Fig. 1(a)] is more reactive than the $|1,0\rangle$ (yellow) and $|1,\pm 1\rangle$ (orange) levels by a factor of ~ 2 . Transferring the entire population from the $|0,0\rangle$ level to the $|1,0\rangle$ level with linearly polarized microwave radiation would thus approximately halve the reaction rate [compare blue and yellow traces in Fig. 1(a)]. The redistribution during the traversal of the field-free region between the coherent state transfer and the reaction zone might randomize the M_J value of the $J = 1$ level [Fig. 1(d)], which would also approximately halve the rate (orange-yellow dashed line). The mechanism presented in Fig. 1 is general and expected to be efficient whenever the capture rates are influenced by long-range interactions involving ions and molecules. In these cases, the rate coefficients are indeed expected to be strongly state dependent [15,18,35], as verified in a growing number of ion-molecule reactions [11,25,31–34].

This state specificity makes the mechanism presented in Fig. 1 a clear example of nonthermal microwave-assisted chemistry, a topic that is discussed controversially in the chemical literature [36–42]. Whereas it is broadly accepted that heating by microwave radiation enhances reaction rates, experimentally proven mechanisms for nonthermal effects of microwaves on reaction rates are lacking. Simple arguments indeed suggest that dielectric heating at the typical 2.45 GHz frequency of commonly used microwave ovens and reactors is not likely to lead to nonthermal effects. Instead, reaction control through selective rotational excitation and molecule orientation represent plausible schemes [43,44]. Experimental conditions favorable for such control would require (i) low temperatures with significant population of only very few rotational levels and (ii) reactions with rate coefficients exhibiting a strong rotational-state dependence through long-range interactions. Both conditions are met in low-temperature capture reactions between ions and molecules having permanent dipole and/or quadrupole moments [14–16,32,45], as discussed in the context of the mechanism presented in Fig. 1.

We report here on a quantitative study of microwave-controlled cold ion-molecule chemistry with the example of the $\text{He}^+ + \text{CO}$ reaction. This reaction has been studied experimentally at temperatures and collision energies in the range between ~ 100 mK and ~ 10 K and the rotational-state-specific capture rate coefficients depicted in Fig. 1 have been derived from the analysis of low-temperature reaction rate coefficients [33] using a rotationally adiabatic capture model [15,16,32]. Following this early work, we use the Rydberg-merged-beam approach to cold ion-molecule chemistry [23,32] to reach the low-temperature conditions necessary for the efficient reactivity control through microwave fields. Specifically, we investigate the reaction $\text{He}(n) + \text{CO} \rightarrow \text{He} + \text{C}(n') + \text{O}$ at low collision

energies, for which we have demonstrated experimentally that the Rydberg electron acts as a spectator to the ion-molecule reaction taking place within its orbit by verifying (i) that the reaction rates are independent of n and (ii) that the Rydberg electron is not affected by the reaction, i.e., that $n = n'$ [46]. The ion-molecule reaction $\text{He}^+ + \text{CO} \rightarrow \text{He} + \text{C}^+ + \text{O}$ is a dissociative charge-transfer process taking place at close-to-capture-limited rates, as established in earlier work [33,47–51].

The experimental setup, consisting of four differentially pumped vacuum chambers, is depicted schematically in Fig. 2 and has been described in Ref. [32]. Here, we emphasize the aspects pertaining to the microwave control of the reactivity. A rotationally cold ($T_{\text{rot}} \approx 3$ K) sample of CO is generated in a supersonic beam of a (80:20) mixture of He and CO using a valve thermalized at 190 K and releasing short (duration ~ 20 μs) gas pulses at a repetition rate of 25 Hz. This beam, with initial velocity of ~ 1050 m/s, is merged with a translationally cold and velocity-tunable beam of $\text{He}(n = 35)$ Rydberg atoms using a curved Rydberg-Stark deflector [25,52,53]. The $\text{He}(n = 35)$ atoms are produced by photoexcitation (wavelength ≈ 260 nm) of metastable $(1s)^1(2s)^1\ ^3S_1$ He atoms generated in an electric discharge located near the orifice of a short-pulse cryogenic valve ($T_{\text{valve}} = 100$ K). Before reaching the reaction region, the short CO-gas pulses propagate over a distance of ~ 60 cm, which ensures a large spatial dispersion in the y direction. As a result, the small cloud (diameter ~ 1 mm) of $\text{He}(n)$ atoms only interacts with neutral reactants in a narrow velocity class, and a collision-energy resolution of $\sim k_B \times 200$ mK is achieved near $E_{\text{coll}} = 0$ [25,52]. Reactions between the He^+ ion core and the CO molecules located within the Rydberg-electron orbit are monitored in the reaction zone by ion time-of-flight (TOF) mass spectrometry. The Rydberg electron acts as a spectator and remains attached to the C^+ reaction product until detection by pulsed-field ionization and extraction of the C^+ ions toward a microchannel-plate (MCP) detector, as discussed in detail in Ref. [46].

Microwaves resonant with the $|0,0\rangle - |1,0\rangle$ transition in the $X^1\Sigma^+$ ($v = 0$) vibronic ground state of CO at ~ 115.2712 GHz are used to induce a coherent population transfer. The microwaves are generated with an rf synthesizer (Anritsu MG3692A) driving a multiplication-amplification chain ($\times 12$, Virginia Diodes WR 6.5, power ≈ 4.5 mW). They are pulsed using an absorptive attenuator, amplified to a peak power of ~ 26.5 mW with a D -band power amplifier and emitted through a conical horn. The microwave radiation has a Gaussian spatial intensity profile and is linearly polarized along the z direction (see Fig. 2). A Teflon lens (diameter of 8 cm, $f = 10.3$ cm, thickness 2.8 cm) positioned ~ 10 cm away from the molecular beam focuses the microwave beam to a $1/e^2$ waist radius of ~ 1.2 cm on the axis of the CO beam in a perpendicular arrangement. The rotational-state population of the CO

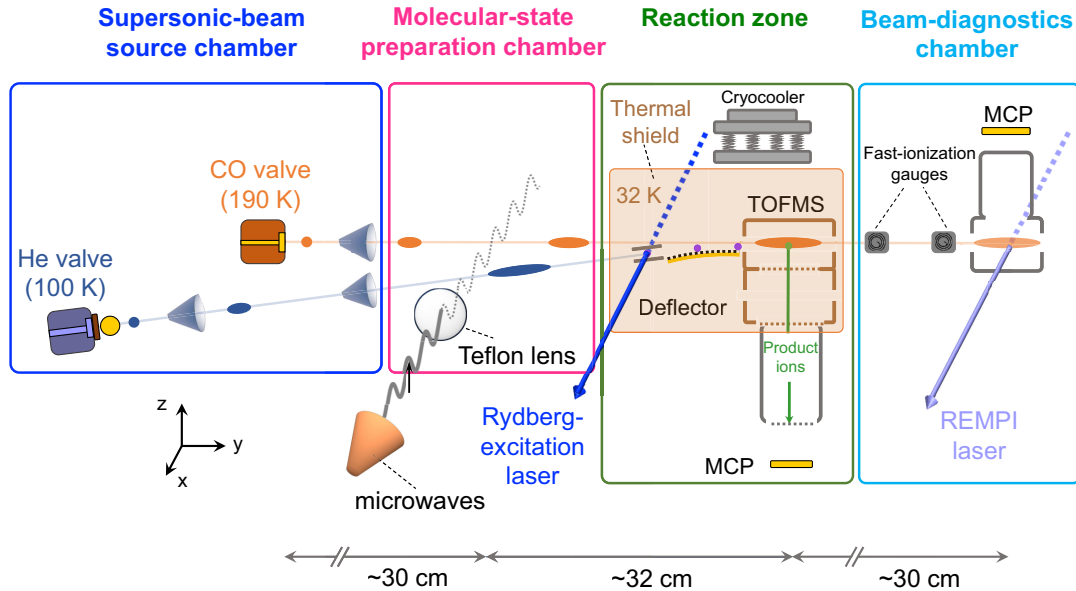


FIG. 2. Schematic representation of the Rydberg-merged-beam setup used to study the effect of microwave-controlled cold ion-molecule chemistry. See text for details.

beam is characterized by $(2 + 1)$ resonance-enhanced multiphoton ionization (REMPI) from the ground vibronic state via the $E^1\Pi$ ($v = 0, J'$) intermediate state [54] in the beam-diagnostics chamber. The REMPI spectra are recorded using the frequency-tripled output of a tunable pulsed Nd:YAG-pumped dye laser (wavelength ~ 215 nm, bandwidth 0.05 cm^{-1} , pulse energy ~ 150 μJ) and the observed transitions correspond to two-photon transitions connecting the ground-state rotational levels populated in the beam to rotational levels of the electronically excited E ($v = 0$) state of CO, which are ionized by a third photon of the same frequency. The beam-diagnostics chamber also contains two fast-ionization gauges for beam-velocity measurements [31].

Figure 3 describes how we quantify the microwave-induced population transfer by recording $(2 + 1)$ REMPI spectra of the CO sample. These spectra consist of five $\Delta J = J' - J''$ branches with $\Delta J = 0$ (Q), ± 1 (R and P), and ± 2 (S and O) labeled in Fig. 3(a) by the value of the ground-state rotational quantum number J'' in parentheses [54]. The positive and negative black traces in Fig. 3(a) correspond to the REMPI spectrum of CO recorded without the microwave field and the spectrum calculated using the program PGOPHER [55] for a population ratio between the $J = 1$ and 0 levels corresponding to a rotational temperature of 3 K, respectively. The occupation probabilities of the $J = 0$ [(62 $^{+11}_8$)%], $J = 1$ [(30 $^{+6}_8$)%], and $J = 2$ [(9 $^{+2}_3$)%] levels inferred from the comparison of the measured and calculated intensities are presented on the left side of Fig. 3(d). To optimize the population transfer, the laser frequency is set to the $S(0)$ line and the frequency and duration of the microwave pulse are adjusted to minimize

its intensity. Under π -pulse conditions, the $J = 1 \leftarrow J = 0$ transition appears as a 67-kHz-wide (full width at half maximum) dip in the CO⁺ REMPI signal at a frequency of 115.271 188(3)_{stat}(25)_{sys} GHz, in agreement with previous measurements of this transition [56,57]. The systematic uncertainty in the transition frequency is dominated by a possible deviation from 90° of the crossing angle between the microwave and molecular beams. Varying the microwave-pulse duration at the resonant frequency [Fig. 3(c)] leads to damped Rabi oscillations, where the population in the $J = 1$ state evolves according to

$$P_{J=1} = \frac{1}{2}[1 - \cos(\Omega t) \exp(-t/T_2)], \quad (1)$$

with $\Omega = 2\pi \times (0.042 \pm 0.001)$ MHz, $T_2 = 26 \pm 2$ μs , and a maximal population transfer of $(88 \pm 0.6)\%$ at 13 μs . This information can be used to extract the CO rotational-state population at the optimal transfer, as displayed on the right side of Fig. 3(d), i.e., $(16 \pm 1)\%$ in $J = 0$, $(75^{+4}_3)\%$ in $J = 1$, and $(9^{+2}_3)\%$ in $J = 2$. Calculating the REMPI spectrum with these populations leads to the blue inverted spectrum in Fig. 3(a), which closely reproduces the REMPI spectrum measured at optimal population transfer.

The C⁺ product-ion signal from the He⁺ + CO reaction is directly proportional to the state-averaged capture rate coefficient. The inhibition of the reaction by the microwave π pulse can thus be directly observed by comparing the C⁺ signal in the TOF mass spectra obtained for resonant (blue trace in the inset of Fig. 4) and far-detuned (black trace) microwave radiation. The comparison demonstrates an inhibition

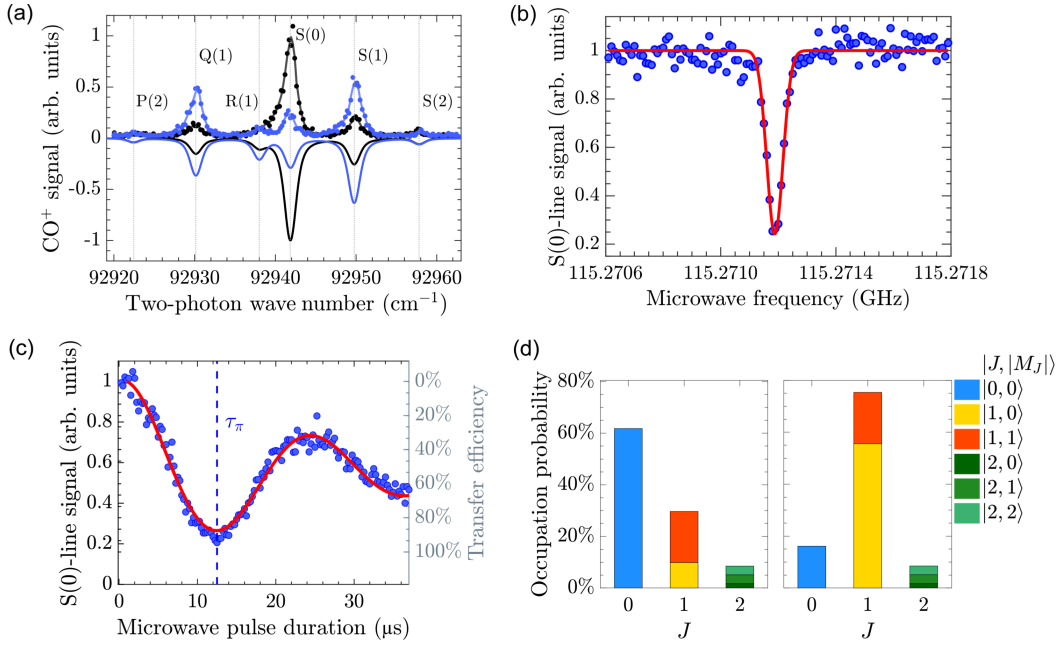


FIG. 3. (a) Comparison of the experimental (dots and three-point running average) and calculated (inverted intensity scale) $(2+1)$ REMPI spectra of the $E^1\Pi(v=0, J') \leftarrow X^1\Sigma^+(v=0, J'')$ two-photon transition of CO recorded in a cold ($T_{\text{rot}} \approx 3$ K) supersonic beam after applying a far-off-resonant microwave pulse (black) and a microwave pulse of the same duration and power but resonant with the $J=1 \leftarrow J=0$ pure-rotational transition in the $X^1\Sigma^+(v=0)$ ground state of CO (blue). (b) Microwave spectrum of the $J=1 \leftarrow J=0$ transition of CO recorded as ion-dip spectrum on the $S(0)$ REMPI transition with the fitted line profile (red line). (c) Observed (blue dots) and fitted (red line) Rabi oscillation in the $J=0$ population as a function of the microwave-pulse duration. The dashed line indicates the pulse duration corresponding to the optimal coherent population transfer (π pulse). (d) Occupation probabilities of the $J=0-2$ rotational levels of CO determined after optimal (right) and without (left) microwave-induced population transfer (see text).

$$\eta = 1 - \frac{k_{\text{mw}}}{k} \quad (2)$$

of the reaction rate by $(40.4^{+2.7}_{-3.9})\%$ at $E_{\text{coll}}/k_{\text{B}} \approx 0$ K. In Eq. (2), k_{mw}/k is the ratio of the rates observed with resonant (k_{mw}) and with detuned (k) microwave frequencies. The reaction inhibitions observed at collision energies of $\sim k_{\text{B}} \times 3$ K and $\sim k_{\text{B}} \times 10$ K are $(30.2 \pm 3)\%$ and $(27.5^{+5.6}_{-4.6})\%$, respectively (see Fig. 4). The blue line in Fig. 4 depicts the reaction inhibition obtained as a weighted average of the calculated state-specific capture rate coefficients [see Fig. 1(a)] using as weights the measured populations of the $J=0-2$ levels, considering the experimental collision-energy resolution, and assuming complete randomization of the M_J components of the $J=1$ level after the coherent microwave-driven population transfer. The blue-shaded area represents the uncertainty in the calculated value of η , which originates from the uncertainties in the measured population of the rotational levels (see above).

For comparison, the red line in Fig. 4 depicts the reaction inhibition calculated assuming that the population initially transferred to the $J=1, M_J=0$ level is not redistributed to the other M_J components, corresponding to the situation depicted in Fig. 1(c). The calculations follow the procedure described in Ref. [33]. In brief, $|J, M_J\rangle$

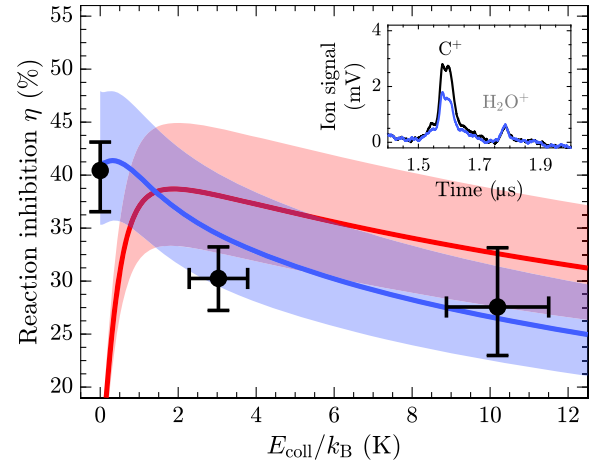


FIG. 4. Microwave-induced inhibition of the $\text{He}^+ + \text{CO} \rightarrow \text{He} + \text{C}^+ + \text{O}$ reaction as a function of the collision energy, obtained experimentally (black dots) and calculated assuming coherent transfer to the $|J=1, M_J=0\rangle$ state (red line) followed by M_J randomization in the $J=1$ level (blue line). The vertical error bars and shaded areas represent the uncertainties, and the horizontal error bars correspond to the range of collision energies probed experimentally. Inset: ion time-of-flight mass spectrum of the $\text{He}^+ + \text{CO}$ reaction mixture recorded after application of a far-off-resonant microwave pulse (black) and a microwave pulse resonant with the $J=1 \leftarrow J=0$ rotational transition of CO $X^1\Sigma^+(v=0)$ (blue).

rotational-state-dependent rate coefficients are determined using an adiabatic capture model based on the earlier work of Clary *et al.* [15,17] and Troe [16], which considers the long-range electrostatic attraction between the charge of the ion and the electric dipole and quadrupole moments of the CO molecules. The collision-energy-dependent rate constant is then obtained as a weighted sum of contributions from the populated CO rotational levels. The large discrepancy at $E_{\text{coll}}/k_{\text{B}} \approx 0$ between the inhibition calculated under this assumption and the experimentally observed inhibition suggests that, under our experimental conditions, M_J is randomized in the $J = 1$ level after the coherent population transfer, corresponding to the situation depicted in Fig. 1(d). We interpret the randomization of M_J as arising from a change in quantization axis. During the microwave-induced rotational-excitation of the CO molecules, the quantization (z) axis corresponds to the polarization of the microwave radiation. In the reaction zone, which is separated from the microwave-excitation region by a field-free flight region where depolarization can take place because of uncontrolled stray fields, the quantization axis of the reacting CO molecules is given by the electric field emanating from the nearest He^+ ion core.

These results demonstrate with the example of the $\text{He}^+ + \text{CO}$ reaction the possibility to inhibit an ion-molecule reaction using microwave fields resonant with pure-rotational transitions of the molecule. Specifically, the reaction was slowed down by coherent population transfer from the ground $J = 0$ to the first excited $J = 1$ rotational level. From the excellent agreement between the calculated and the measured inhibition, we conclude that the mechanism proposed to account for the microwave control of reactivity (see Fig. 1) is valid. The contribution of thermal effects caused by heating the sample with microwaves was excluded in control measurements with off-resonant microwave fields of the same power. The results provide unambiguous evidence for a mechanism of nonthermal microwave-induced reactivity control and thus represent an important contribution to the field of microwave-assisted chemistry [36–44]. Although we used the control scheme to inhibit the reaction, it can be implemented as a general reactivity-control scheme to either enhance, suppress, or tune the rate of a reaction by appropriately choosing the length of the microwave pulse and the phase of the Rabi oscillation of the rotational population. Whereas the scheme is demonstrated here using a sample cooled to the ground rotational level, it would function equally well for a molecule sample prepared in a selected rotational level, e.g., using a strong-field state deflector [58] or electrostatic multipole lenses [59].

Acknowledgments—We thank Dr. Gunther Wichmann, Dr. Raphaël Hahn, and David Schlander for fruitful discussions. This work is supported by the Swiss National Science Foundation (Grant No. 200020B 200478).

- [1] T. Langen, G. Valtolina, D. Wang, and J. Ye, Quantum state manipulation and cooling of ultracold molecules, *Nat. Phys.* **20**, 702 (2024).
- [2] J. R. Li, K. Matsuda, C. Miller, A. N. Carroll, W. G. Tobias, J. S. Higgins, and J. Ye, Tunable itinerant spin dynamics with polar molecules, *Nature (London)* **614**, 70 (2023).
- [3] S. L. Cornish, M. R. Tarbutt, and K. R. A. Hazzard, Quantum computation and quantum simulation with ultracold molecules, *Nat. Phys.* **20**, 730 (2024).
- [4] T. S. Roussy, L. Caldwell, T. Wright, W. B. Cairncross, Y. Shagam, K. B. Ng, N. Schlossberger, S. Y. Park, A. Wang, J. Ye, and E. A. Cornell, An improved bound on the electron's electric dipole moment, *Science* **381**, 46 (2023).
- [5] D. DeMille, N. R. Hutzler, A. M. Rey, and T. Zelevinsky, Quantum sensing and metrology for fundamental physics with molecules, *Nat. Phys.* **20**, 741 (2024).
- [6] S. Willitsch, *Chemistry with Controlled Ions* (John Wiley & Sons, Inc., New York, 2017), pp. 307–340.
- [7] *Cold Chemistry: Molecular Scattering and Reactivity Near Absolute Zero*, edited by O. Dulieu and A. Osterwalder (The Royal Society of Chemistry, Cambridge, 2017).
- [8] J. Toscano, H. J. Lewandowski, and B. R. Heazlewood, Cold and controlled chemical reaction dynamics, *Phys. Chem. Chem. Phys.* **22**, 9180 (2020).
- [9] C. R. Markus, O. Asvany, T. Salomon, P. C. Schmid, S. Brünken, F. Lipparini, J. Gauss, and S. Schlemmer, Vibrational excitation hindering an ion-molecule reaction: The $\text{c-C}_3\text{H}_2^+ - \text{H}_2$ collision complex, *Phys. Rev. Lett.* **124**, 233401 (2020).
- [10] Y. Liu and K. K. Ni, Bimolecular chemistry in the ultracold regime, *Annu. Rev. Phys. Chem.* **73**, 73 (2022).
- [11] K. Höveler, J. Deiglmayr, J. A. Agner, R. Hahn, V. Zhelyazkova, and F. Merkt, Observation of quantum capture in an ion-molecule reaction, *Phys. Rev. A* **106**, 052806 (2022).
- [12] E. Herbst and W. Klemperer, The formation and depletion of molecules in dense interstellar clouds, *Astrophys. J.* **185**, 505 (1973).
- [13] E. Herbst, The chemistry of interstellar space, *Chem. Soc. Rev.* **30**, 168 (2001).
- [14] D. Smith, The ion chemistry of interstellar clouds, *Chem. Rev.* **92**, 1473 (1992).
- [15] D. C. Clary, D. Smith, and N. G. Adams, Temperature dependence of rate coefficients for reactions of ions with dipolar molecules, *Chem. Phys. Lett.* **119**, 320 (1985).
- [16] J. Troe, Statistical adiabatic channel model for ion-molecule capture processes, *J. Chem. Phys.* **87**, 2773 (1987).
- [17] D. C. Clary, Fast chemical reactions: Theory challenges experiment, *Annu. Rev. Phys. Chem.* **41**, 61 (1990).
- [18] J. Troe, Statistical adiabatic channel model for ion-molecule capture processes. II. Analytical treatment of ion-dipole capture, *J. Chem. Phys.* **105**, 6249 (1996).
- [19] E. I. Dashevskaya, I. Litvin, E. E. Nikitin, and J. Troe, Rates of complex formation in collisions of rotationally excited homonuclear diatoms with ions at very low temperatures: Application to hydrogen isotopes and hydrogen-containing ions, *J. Chem. Phys.* **122**, 184311 (2005).
- [20] E. I. Dashevskaya, I. Litvin, E. E. Nikitin, and J. Troe, Relocking of intrinsic angular momenta in collisions of diatoms with ions: Capture of H_2 ($j = 0, 1$) by H_2^+ , *J. Chem. Phys.* **145**, 244315 (2016).

- [21] R. Wester, Radiofrequency multipole traps: Tools for spectroscopy and dynamics of cold molecular ions, *J. Phys. B* **42**, 154001 (2009).
- [22] S. Willitsch, M. T. Bell, A. D. Gingell, and T. P. Softley, Chemical applications of laser- and sympathetically-cooled ions in ion traps, *Phys. Chem. Chem. Phys.* **10**, 7200 (2008).
- [23] P. Allmendinger, J. Deiglmayr, O. Schullian, K. Höveler, J. A. Agner, H. Schmutz, and F. Merkt, New method to study ion-molecule reactions at low temperatures and application to the $\text{H}_2^+ + \text{H}_2 \rightarrow \text{H}_3^+ + \text{H}$ reaction, *Chem. Phys. Chem.* **17**, 3596 (2016).
- [24] A. D. Dörfler, P. Eberle, D. Koner, M. Tomza, M. Meuwly, and S. Willitsch, Long-range versus short-range effects in cold molecular ion-neutral collisions, *Nat. Commun.* **10**, 5429 (2019).
- [25] V. Zhelyazkova, F. B. V. Martins, J. A. Agner, H. Schmutz, and F. Merkt, Ion-molecule reactions below 1 K: Strong enhancement of the reaction rate of the ion-dipole reaction $\text{He}^+ + \text{CH}_3\text{F}$, *Phys. Rev. Lett.* **125**, 263401 (2020).
- [26] O. A. Krohn, K. J. Catani, S. P. Sundar, J. Greenberg, G. da Silva, and H. J. Lewandowski, Reactions of acetonitrile with trapped, translationally cold acetylene cations, *J. Phys. Chem. A* **127**, 5120 (2023).
- [27] O. A. Krohn and H. J. Lewandowski, Cold ion-molecule reactions in the extreme environment of a Coulomb crystal, *J. Phys. Chem. A* **128**, 1737 (2024).
- [28] A. Kilaj, H. Gao, D. Rösch, U. Rivero, J. Küpper, and S. Willitsch, Observation of different reactivities of para and ortho-water towards trapped diazenylium ions, *Nat. Commun.* **9**, 2096 (2018).
- [29] L. S. Petralia, A. Tsikritea, J. Loreau, T. P. Softley, and B. R. Heazlewood, Strong inverse kinetic isotope effect observed in ammonia charge exchange reactions, *Nat. Commun.* **11**, 173 (2020).
- [30] O. A. Krohn, K. J. Catani, J. Greenberg, S. P. Sundar, G. da Silva, and H. J. Lewandowski, Isotope-specific reactions of acetonitrile (CH_3CN) with trapped, translationally cold CCl^+ , *J. Chem. Phys.* **154**, 074305 (2021).
- [31] R. Hahn, D. Schlender, V. Zhelyazkova, and F. Merkt, Opposite effects of the rotational and translational energy on the rates of ion-molecule reactions near 0 K: The $\text{D}_2^+ + \text{NH}_3$ and $\text{D}_2^+ + \text{ND}_3$ reactions, *Phys. Rev. X* **14**, 011034 (2024).
- [32] V. Zhelyazkova, F. B. V. Martins, J. A. Agner, H. Schmutz, and F. Merkt, Multipole-moment effects in ion-molecule reactions at low temperatures: Part I—ion-dipole enhancement of the rate coefficients of the $\text{He}^+ + \text{NH}_3$ and $\text{He}^+ + \text{ND}_3$ reactions at collisional energies $E_{\text{coll}}/k_{\text{B}}$ near 0 K, *Phys. Chem. Chem. Phys.* **23**, 21606 (2021).
- [33] F. B. V. Martins, V. Zhelyazkova, and F. Merkt, Effects of the charge-dipole and charge-quadrupole interactions on the $\text{He}^+ + \text{CO}$ reaction rate coefficients at low collision energies, *New J. Phys.* **24**, 113003 (2022).
- [34] V. Zhelyazkova, F. B. V. Martins, S. Schilling, and F. Merkt, Reaction of an ion and a free radical near 0 K: $\text{He}^+ + \text{NO} \rightarrow \text{He} + \text{N}^+ + \text{O}$, *J. Phys. Chem. A* **127**, 1458 (2023).
- [35] S. C. Smith and J. Troe, Statistical modeling of ion-molecule electrostatic capture, *J. Chem. Phys.* **97**, 5451 (1992).
- [36] G. Majetich and R. Hicks, Applications of microwave-accelerated organic synthesis, *Radiat. Phys. Chem.* **45**, 567 (1995).
- [37] S. A. Galema, Microwave chemistry, *Chem. Soc. Rev.* **26**, 233 (1997).
- [38] A. de la Hoz, A. Díaz-Ortiz, and A. Moreno, Microwaves in organic synthesis. Thermal and non-thermal microwave effects, *Chem. Soc. Rev.* **34**, 164 (2005).
- [39] C. O. Kappe, B. Pieber, and D. Dallinger, Microwave effects in organic synthesis: Myth or reality?, *Angew. Chem., Int. Ed.* **52**, 1088 (2013).
- [40] P. Prieto, A. de la Hoz, A. Díaz-Ortiz, and A. M. Rodríguez, Understanding MAOS through computational chemistry, *Chem. Soc. Rev.* **46**, 431 (2017).
- [41] E. Petricci, E. Cini, and M. Taddei, Metal catalysis with microwaves in organic synthesis: A personal account, *Eur. J. Org. Chem.* **2020**, 4435 (2020).
- [42] M. Gladovic, C. Oostenbrink, and U. Bren, Could microwave irradiation cause misfolding of peptides?, *J. Chem. Theory Comput.* **16**, 2795 (2020).
- [43] A. Miklavc, Strong acceleration of chemical reactions occurring through the effects of rotational excitation on collision geometry, *Chem. Phys. Chem.* **2**, 552 (2001).
- [44] U. Bren, A. Kržan, and J. Mavri, Microwave catalysis through rotationally hot reactive species, *J. Phys. Chem. A* **2**, 166 (2008).
- [45] C.-Y. Ng, M. Baer, I. Prigogine, and S. A. Rice, *State-Selected and State-To-State Ion-Molecule Reaction Dynamics, Part I. Experiment*, Advances in Chemical Physics Vol. 82 (John Wiley & Sons, Inc., New York, 1992).
- [46] F. B. V. Martins, V. Zhelyazkova, Ch. Seiler, and F. Merkt, Cold ion chemistry within a Rydberg-electron orbit: Test of the spectator role of the Rydberg electron in the $\text{He}(n) + \text{CO} \rightarrow \text{C}(n') + \text{O} + \text{He}$ reaction, *New J. Phys.* **23**, 095011 (2021).
- [47] V. G. Anicich, J. B. Laudenslager, W. T. Huntress, Jr., and J. H. Futrell, Product distributions for some thermal energy charge transfer reactions of rare gas ions, *J. Chem. Phys.* **67**, 4340 (1977).
- [48] W. Lindinger, D. L. Albritton, and F. C. Fehsenfeld, Energy dependence of the reaction of He^+ with NH_3 , *J. Chem. Phys.* **62**, 4957 (1975).
- [49] R. C. Bolden, R. S. Hemsworth, M. J. Shaw, and N. D. Twiddy, Measurements of thermal-energy ion-neutral reaction rate coefficients for rare-gas ions, *J. Phys. B: At. Mol. Opt. Phys.* **3**, 45 (1970).
- [50] F. C. Fehsenfeld, A. L. Schmeltekopf, P. D. Goldan, H. I. Schiff, and E. E. Ferguson, Thermal energy ion-neutral reaction rates. I. Some reactions of helium ions, *J. Chem. Phys.* **44**, 4087 (1966).
- [51] B. R. Rowe, J. B. Marquette, G. Dupeyrat, and E. E. Ferguson, Reactions of He^+ and N^+ ions with several molecules at 8 K, *Chem. Phys. Lett.* **113**, 403 (1985).
- [52] P. Allmendinger, J. Deiglmayr, J. A. Agner, H. Schmutz, and F. Merkt, Surface-electrode decelerator and deflector for Rydberg atoms and molecules, *Phys. Rev. A* **90**, 043403 (2014).
- [53] V. Zhelyazkova, M. Žeško, H. Schmutz, J. A. Agner, and F. Merkt, Fluorescence-lifetime-limited trapping of Rydberg helium atoms on a chip, *Mol. Phys.* **117**, 2980 (2019).

- [54] S. R. Mackenzie, E. J. Halse, E. Gordon, D. Rolland, and T. P. Softley, Pulsed-field ionization spectroscopy of CO via the E $^1\Pi$ state and NO via the B $^2\Pi$ state, *Chem. Phys.* **209**, 127 (1996).
- [55] C. M. Western, PGOPHER: A program for simulating rotational, vibrational and electronic spectra, *J. Quant. Spectrosc. Radiat. Transfer* **186**, 221 (2017).
- [56] B. Rosenblum, A. H. Nethercot, and C. H. Townes, Isotopic mass ratios, magnetic moments and the sign of the electric dipole moment in carbon monoxide, *Phys. Rev.* **109**, 400 (1958).
- [57] G. Winnewisser, S. P. Belov, T. Klaus, and R. Schieder, Sub-doppler measurements on the rotational transitions of carbon monoxide, *J. Mol. Spectrosc.* **184**, 468 (1997).
- [58] L. Ploenes, P. Straňák, H. Gao, J. Küpper, and S. Willitsch, A novel crossed-molecular-beam experiment for investigating reactions of state- and conformationally selected strong-field-seeking molecules, *Mol. Phys.* **119**, e1965234 (2021).
- [59] D. H. Parker and R. B. Bernstein, Oriented molecule beams via the electrostatic hexapole: Preparation, characterization, and reactive scattering, *Annu. Rev. Phys. Chem.* **40**, 561 (1989).